Optimization of Reaction Conditions for High Yield Synthesis of Carbon Nanotube Bundles by Low-Temperature Solvothermal Process and Study of their H_2 Storage Capacity

G. Krishnamurthy[*] and Sarika Agarwal

Department of Studies in Chemistry, Bangalore University, Dr. B. R. Ambedkar Veedhi, Bangalore-560001, India
[*]E-mail: krismurg@gmail.com

Synthesis of Carbon Nanotube bundles has been achieved by simple and economical solvothermal procedure at very low temperature of 180 °C. The product yield obtained was about 70-75%. The optimization of reaction conditions for an efficient synthesis of CNTs has been presented. The CNTs are obtained by reduction of hexachlorobenzene in the presence of Na/Ni in cyclohexane. The X-ray diffraction, Fourier transform infrared and Raman spectral studies have inferred us the graphene structure of the products. The CNTs formed as the bundles were viewed on scanning electron microscope, transmission electron microscope and high-resolution transmission electron microscope. These are the multiwalled CNTs with outer diameter of 5-10 nm, the inner diameter 2-4 nm and cross sectional diameter up to 5 nm. Brunauer-Emmett-Teller (BET) based N_2 gas adsorption studies have been made to obtain BET surface area and H_2 storage capacity. Effect of the experimental variables such as reaction temperature, amount of catalyst and the amount of carbon source were investigated. It is found that they affect significantly on the product nature and yield.

Key Words : Solvothermal process, MWCNTs' bundles, Electron microscopy, BET study, H_2 storage

Introduction

There has been increased interest on the shape and dimension oriented synthesis of carbon nanotubes (CNTs), since their discovery by Iijima,[1] in 1991. The sp^2 carbon network formed during reaction in the form of graphene sheets is capable of rolling up to give concentric cylinders of single, double/multiwalled tubes with the dimensions in micro to nano range. These nanotubes are found to possess a variety of interesting physical and chemical properties. These include gas absorption, mechanical strength, electrical, electronic and optical conductance, *etc*. Due to that they find several important applications, [2-4] and hence CNTs have attracted a large number of researchers and entrepreneurs to explore them. For example, carbon nanotubes can be used as, hydrogen storage materials,[5] electrochemical devices,[6] electronic devices, nanotweezers,[7] field emission devices,[8] *etc*.

The very challenging aspect of the CNTs research is to produce them cost effectively in a large scale. Various methods have been developed for the synthesis of carbon nanotubes, including metal catalyzed chemical vapor deposition (CVD),[9,10] arc evaporation,[11] laser ablation of carbon,[12,13] catalytic decomposition[14] and pyrolysis.[15,16] Some of these techniques can produce nanotubes in sizable quantities. However, need of high temperature and reaction time make their manufacturing costs high and still prohibit widespread commercialization. The complex procedure, the catalyst and other production cost have become obstacles' for the CNTs synthesis. Hence, there is much interest in lowering the growth temperature while maintaining high yields. Recent reports indicated that carbon nanotubes could be synthesized from hydrothermal processing[17] or by solid-state metathesis reaction.[18,19] To explore other alternatives, a high and low temperature solvothermal routes have been developed to prepare carbon nanotubes, in which the alkali metals such as Na and K were used as reductants.[20,21]

Xinjun Wang *et al.* (2002)[21] has reported the synthesis of MWCNTs by the solvothermal process by heating at 200 °C for about 27 h. The yield of CNTs obtained was only about 15%. Lee *et al*. has reported the synthesis of carbon materials with a graphitic structure through a Wurtz-like reaction of hexachlorobenzene (HCB) and sodium, but no porous structure was obtained.[22] Jianwei Liu *et al.* (2003) reported[23] the synthesis of MWCNTs by heating at 500 °C for 10 h in about 35% yield. Whenzhang Wang *et al.* (2005) has reported[24] about 20% of CNTs on heating for 72 h but they were not bundles. Qian's group has reported the formation of carbon nanotubes from a similar reaction between HCB and potassium with a mixed catalyst. However, the tubes in this work grew with random orientation and in insignificant amounts.

Here we are reporting the synthesis of bundles of multiwalled carbon nanotubes (MWCNTs) by an efficient procedure compare to the above procedures at much lower temperatures of 180 °C and much higher yield of about 70-75%. The experiments were carried out in the temperature range of 160-220 °C to optimize the reaction conditions. The optimum temperature for the production of CNTs by these experimental conditions is found to be 180 °C. However the

High Yield Synthesis of Carbon Nanotube Bundles

Bull. Korean Chem. Soc. **2013**, Vol. 34, No. 10   3047

lower temperature has not yielded the CNTs and the higher temperatures up to 220 °C have not shown any significant increase in the yields. The products obtained were purified and characterized by various analytical techniques as discussed below. Hydrogen adsorption studies on as obtained and purified carbon nanotubes are discussed by a model based on a hypothetical condensation mechanism and the possible amount of absorbed hydrogen is calculated.
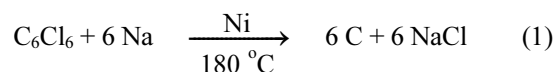
Experimental

Materials and Synthesis Procedure. The materials such as sodium metal, nickel chloride, HCB, cyclohexane, alcohol, hydrochloric acid *etc.*, were obtained from Merck Chemicals. Synthesis of CNTs involves firstly the dehydration of $NiCl_2 \cdot 6H_2O$ by heating at around 220 °C. The dehydrated $NiCl_2$ was dispersed in 30 mL of cyclohexane for about 30 min. 1.0 g Na was added in the form of smaller slices into a stainless steel autoclave having Teflon inner lining. The autoclave was sealed and heated at a temperature 160 to 220 °C for 6 h in different experiments. Then it was cooled to room temperature and about 3.0 g of HCB was added to it and filled with cyclohexane to 2/3 of its capacity. The autoclave was sealed and heated at the temperature range from 160 to 220 °C for 9-10 h. After 10h of heating it was allowed to cool down to room temperature.

The black colored product formed was collected by filtration and washed sequentially with cyclohexane, ethanol, hydrochloric acid (1.0 M) and distilled water to remove the impurities. Finally it was dried at around 100 °C in oven for 6 h. The products formed at 200 °C and 220 °C were almost quite close to that obtained at 180 °C in terms of features and yield. Hence, 180 °C is the optimum and low temperature for solvothermal synthesis of CNTs with considerably good yield and significant dimensions. Also the experiments with various amounts of $NiCl_2$ have been performed keeping the source amount constant to study the effect of the catalyst amount.

Analytical Methods. The X-ray diffraction (XRD) studies were made using a Bruker D8 Advance powder X-ray diffractometer to check the purity, phase structure and crystallanity of the products. The Fourier transform infrared (FTIR) using FTIR 8400S Shimadzu spectrophotometer and Raman spectral studies using Perkin Elmer instrument were made to characterize the graphene materials. The surface morphologies of the samples were observed through JEOL model JSM 6490 LV scanning electron microscope (SEM) and Phillips CS12 model transmission electron microscope (TEM). Further the high resolution transmission electron microscopic (HRTEM) images were taken for more resoled stuctual analysis using JOEL 3011 Microscope. Elemental analysis was performed by Elementar Vario MICRO V1.9.7 analyzer to study the purity and composition of the products. Also, Brunauer-Emmett-Teller (BET) based N_2 gas adsorption studies were made using Micromeritics BET surface area measurement instrument (model ASAP2020).

Results and Discussion

Optimization of Reaction Conditions. In solvothermal experiments, first the metallic sodium pieces are reduced into smaller particles at that reaction temperature with $NiCl_2$. The $NiCl_2$ will be reduced to Ni particles by sodium and deposited over the Na Balls. Smaller Na balls provide high surface area for the Ni particles to disperse on them where Ni particles will act as catalyst for the second step. When HCB is added, metallic Na reduces it to produce free C_2 (or C=C) and sodium chloride in the presence of catalysts. The chemical reaction can be represented as follows:

$$C_6Cl_6 + 6\ Na \xrightarrow[180\ ^oC]{Ni} 6\ C + 6\ NaCl \qquad (1)$$

As the tubular structures cannot be formed successfully without catalyst,[19] the experiments in the absence of catalysts have yielded no expected product. Therefore the experiments were performed in the presence of Ni catalyst, sodium metal in cyclohexane solvent between 160 °C and 220 °C using HCB as the carbon source. However at 160 °C, there were only blackish gray or brown colored foils/lumps were formed without much morphological change. This could be owing to a very rapid reaction between the reactants, such that the sodium slices could not even melt to form spheres at such a temperature.[24] The similar experiment performed at 180 °C were resulted the formation of black carbon having arrays of narrow shaped morphological features, which were later confirmed as the CNTs.

However, the direct reaction of the catalyst with reactants did not bring effective catalysis due to rapid reaction. Hence $NiCl_2$ was first dispersed by stirring and added with sodium to the autoclave. Further the autoclave was sealed and heated at 180 °C temperature for 5-6 h. This process ensures that the catalyst precursor $NiCl_2$ was fully reduced by metallic sodium and as expected that tiny particles of nickel would deposit on the surface of sodium balls. In this step we have not found much difference between 5 h and 6 h of heating because many reports have stuck to heating for 6 h. Hence we are reporting that heating for about 5 h in the first step would be enough. In the second step after 9-10 h of heating the product obtained was containing almost narrow well-ordered arrays/bundles. The experiments were also conducted at 200 °C and 220 °C in the similar manner and almost the very close results were obtained in terms of product yield, features, etc. This reveals the optimum temperature for the production of CNTs by this procedure is 180 °C, which would be the lowest temperature for producing CNTs with considerably good yield and morphologies. Though there are several reports[23,25] on the solvothermal synthesis of CNTs at low temperature, this would be the lowest yielding CNTs of significant dimensions and percentage.
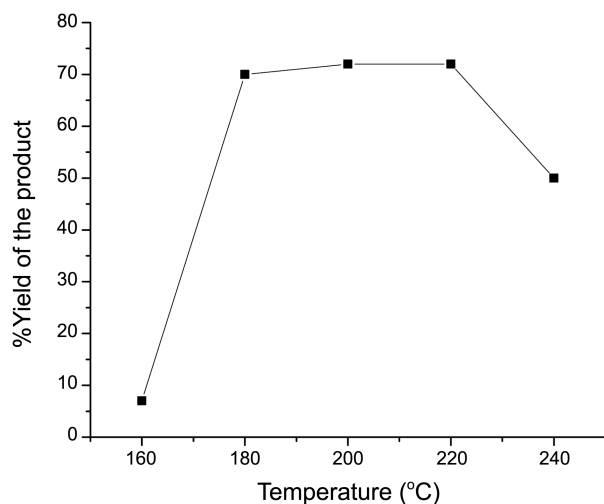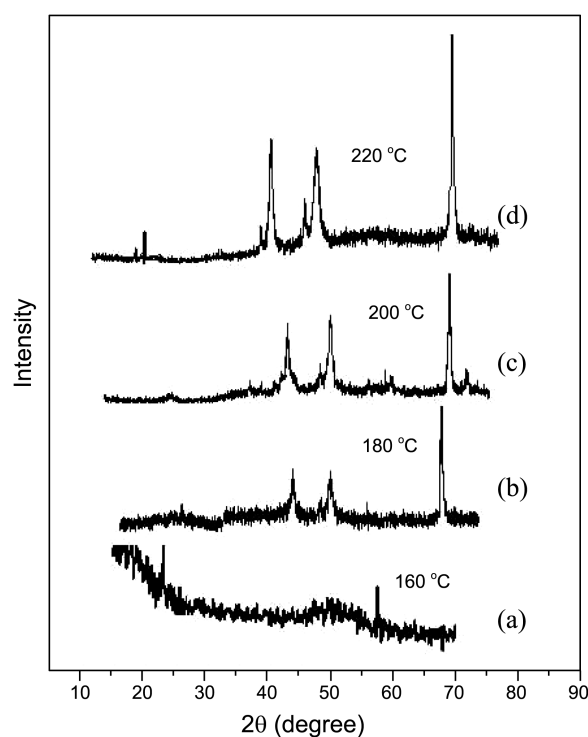
In this work, we had carried out a systematic study of reaction to optimize the reaction conditions for CNT bundles. A number of experiments have been performed, as discussed in Table 1 to optimize reaction conditions by varying

Table 1. Experimental conditions out come data to optimize the synthesis procedure

Sets of run	Amount of catalyst (gm)	Amount of Carbon source (gm)	Temperature (°C)	% yield of the product
1	0.05	1/2/3	160	No CNTs
	0.1	1/2/3		
	0.2	1/2/3		
	0.3	1/2/3		
2	0.05	1/2/3	180	20-35
	0.1	1/2/3		40-70
	0.2	1/2/3		42-70
	0.3	1/2/3		45-75
3	0.05	1/2/3	200	20-25
	0.1	1/2/3		40-55
	0.2	1/2/3		45-70
	0.3	1/2/3		47-72
4	0.05	1/2/3	220	30-32
	0.1	1/2/3		35-40
	0.2	1/2/3		42-55
	0.3	1/2/3		55-70

one parameter while keeping other parameters constant.

The reaction temperature is an important parameter, which influence on the product yield and structure of CNTs (shape and size). Figure 1 presents the impact of temperature on the product yield while maintaining other reaction parameters constant. It has been reported earlier that higher temperature tends to produce a higher carbon yield since it has an immense impact on the activity of metals and carbon containing gases. But excessively higher temperature may result in the agglomeration of catalyst particles and can be tuned as a negative factor for CNTs formation.[26] Therefore a judicious reaction temperature is required to synthesize CNTs in high yield. Figure 2 carries four XRD pattern for CNT samples synthesized at temperatures ranging from 160- 220 °C. Heating at 160 °C has resulted in a brown powder

Figure 1. Plot of product yield (%) as a function of heating temperature.

Figure 2. XRD patterns of CNT samples synthesized at various reaction temperatures.

containing lumps and particles. The XRD of this powder has given weak carbon peaks at $2\theta = 23°$ and $43°$. Prominent carbon peak at $2\theta = 23°$ and a weak peak at $43°$ are attributed to well formed bundles which were observed when the heating was carried at 180 °C. Further rise in heating temperature has shown no significant changes in the yield.

This result is further supported by the SEM images for the samples synthesized at various temperatures. In the Figure 3, the image (a) corresponds to the sample synthesized at 160 °C which does not show CNT bundles. While the images (b), (c) and (d) are correspond to the samples synthesized at 180 °C, 200 °C and 220 °C respectively. These images show the presence of straight and long CNTs' bundles with similar morphologies. This shows that the optimum heating temperature for the synthesis of MWCNTs is about 180 °C. The CNTs content of the product obtained under the best experimental condition is about 70-75%.

Similarly the effect of the amount of Ni catalyst on the experimental outcome also as been studied. The percentage yields have been increased with increase in the catalyst amount up to 0.1 g and further a gradual rise or almost constant trend is observed with further increase in the catalyst amount as it can be seen in the Figure 4. Figure 4 implies the effect of catalyst on the product yield. This inspection suggests that catalyst become more active with a higher metal content as the temperature increased. This happened since the CNTs synthesis was intimately allied with the available carbon source and the active sites of the catalytic metal particles. After reaching a stable level, the carbon yield started to decrease even though the amount of
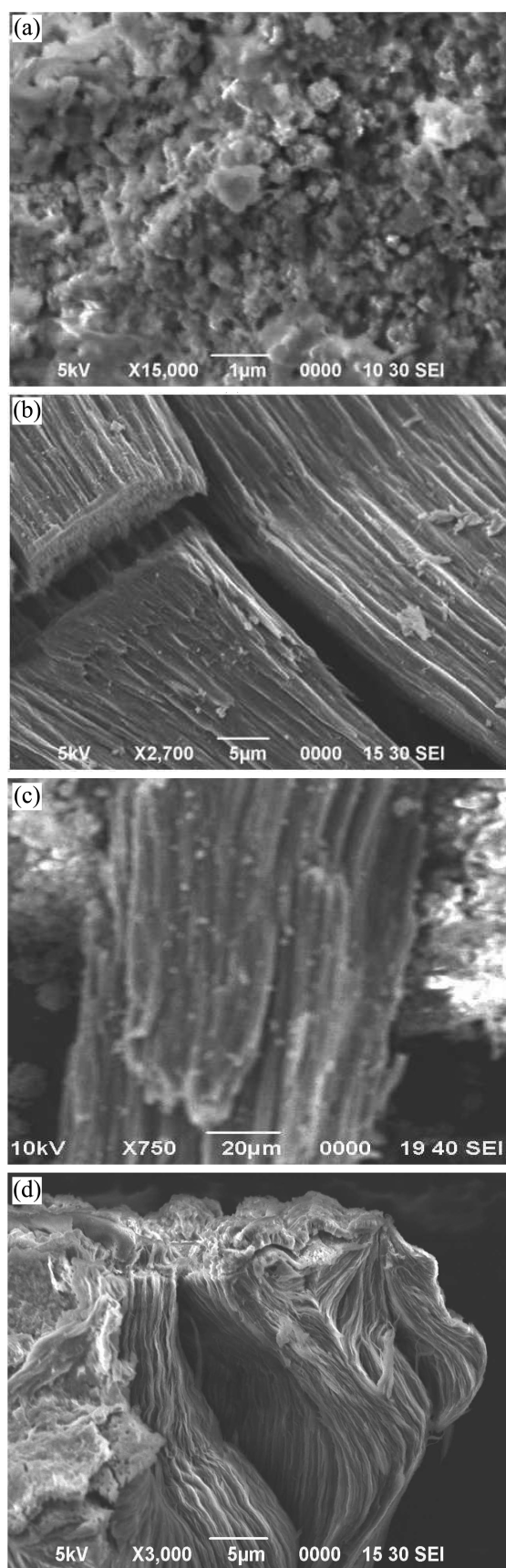
Figure 3. SEM images, (a), (b), (c) and (d) correspond to the as obtained products at various reaction temperatures indicating the bundles of straight CNTs.

Table 2. Optimization criteria for the synthesis of CNTs bundles

Reaction Parameter	Value
Amount of catalyst (gm)	0.1
Amount of carbon source (gm)	3.0
Temperature (°C)	180
Amount of Sodium (gm)	1.0
Product yield (%)	70-75

Figure 4. Plot of percentage yield of product as a function of amount of catalyst.

catalyst increased, because the contact time restricted the available carbon source. The optimized conditions are provided in Table 2.

The purity and phase structure of the products were obtained from XRD studies using the monochromatic high-intensity CuKα radiation (λ = 0.1541874 nm). Figure 5 contains the PXRD pattern (a) of the as-obtained product (at optimum conditions as described in Table 2). The patterns (b) and (c) are the PXRD patterns, after treating CNT
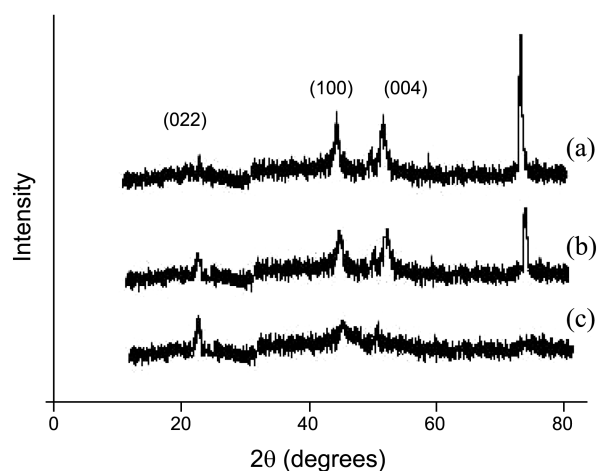

Figure 5. XRD patterns of CNT samples synthesized at optimum conditions in which pattern (a) corresponds to as prepared sample, (b) and (c) are correspond to the samples after washed with HCl (1 M) solution for second and third time respectively.

products with HCl (1 M) solution for second and third time respectively. The washings with more concentrated solutions such as 2 M and 5 M HCl was found to etch the CNTs. Pattern (a) has the peaks at 2θ values, 23° and 45° which are attributed to sp^2 carbon of graphene correspond to (002) and (100) plane respectively. The remaining peaks can be assigned to Ni metal. No other characteristic graphitic diffraction peaks appear at higher reflection angles as in other reports. The appearance of these peaks even though with a little bit of noise, implies the structures are crystalline to the greater extent. However the graphitic peaks are appearing as prominent after repeated treatment with acid solution as the Ni content disappear from carbon powder (Figure 5 patterns b and c).

Figure 6 is the Raman spectrum of the as obtained product. The Raman spectral runs were made at 1064 nm wavelength using FT-Raman equipped with liquid nitrogen cooled Ge detector. Raman spectrum of MWCNTs with large diameter is similar to the SWCNTs Raman spectrum. The spectrum of our CNT product has two bands at around 1580 cm^{-1} (G-Band) and 1355 cm^{-1} (D-Band). These bands correspond to the symmetric E_{2g} mode of vibrations of sp^2 bonded carbon atoms in 2D hexagonal lattice as in the case of graphite and vibrations of carbon atoms with dangling bonds in plane terminations of disordered graphite respectively. MWCNTs are composed of series of concentric graphene sheets rolled in a cylindrical form with an inner tube diameter ~0.34 nm to outer tube diameter ~0.50 nm. And because of the large outer tube diameter of MWCNTs, no RBM signal observed in their Raman spectra. A low energy RBM signal at 248/$d_t$cm^{-1} (where d_t is tube diameter) is the characteristic signal for SWCNTs. Position and intensity of our Raman peaks are in good agreement with theoretical calculations for SWCNTs, which shows that the vibration structure of MWCNTs is quite similar to SWCNTs.[27] Along with RBM band the integrated intensity ratio between the D and G band (I_D/I_G) also allows distinguish between MWCNTs and SWCNTs. A very less difference between the intensity of G band and D band in Figure 6 indicates the presence of MWCNTs in our as obtained product. While SWCNTs show higher difference between intensities of D
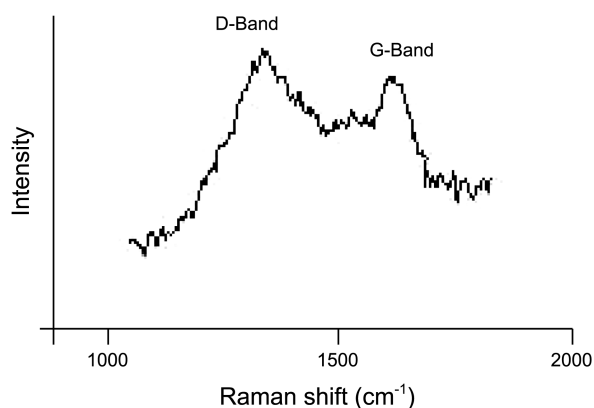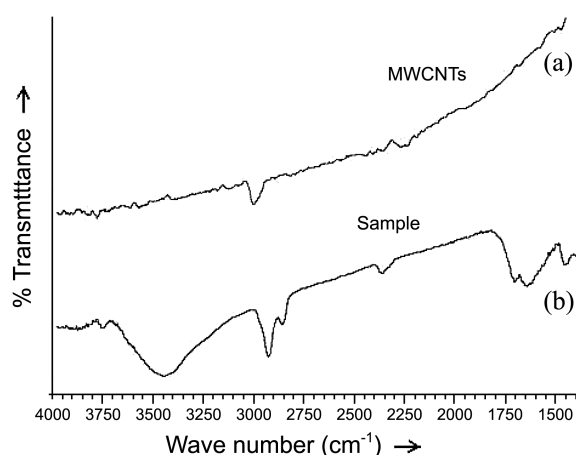

Figure 7. FTIR spectrum of as synthesized product.

and G band. The I_D/I_G also indicates the quality of the sample. Higher value of I_D/I_G (0.9) indicates the high quantity of structural defects because of MWCNTs multiple graphite layers also support the synthesis of MWCNTs for our samples. Figure 7 shows the IR spectra (a) and (b). Spectrum (a) corresponds to the commercial sample of MWCNTs. The spectrum presents strong bands in the region 1600-1345 cm^{-1} and in between 2300-2500 cm^{-1}. Spectrum (b) is correspond to our sample which also shows the bands in the same regions. Strong bands are evident in the region 1710-1345 cm^{-1}, in particular at 1344, 1454, 1540, 1600, 1700 cm^{-1} for MWCNTs.

Figure 3(b), (c) and (d) shows the scanning electron microscopic (SEM) images of the carbon powders. The SEM images display a large quantity of long and well ordered arrays or bundles of carbon tubes like structures. Some of the tubes like structures on the surface of the bundles are appeared like opened channels, which could be due to some hard mechanical operations by friction or abrasion. This also could be attributed to acid etching during post treatment of these products. From the SEM images it can also be seen a kind of layer on the surface at some region, which could be a layer of some unconverted reactant material (impurity). This layer has disappeared after post treatment of the product. These structures were further confirmed by taking the TEM and HRTEM images.

Figure 8, in which (a) and (b) are the TEM images obtained by operating at 100 kV. The images show the bundles and tubular structures of carbon powders, which have the sizes in the nanometer scale and hence these are ascertained as the carbon nanotubes. Further these CNTs are viewed through HRTEM with an instrument at the accelerating voltage of 300 kV. The HRTEM images (Figure 9(a) and (b)) show the multiwalled CNTs with outer diameter of about 5-9 nm, the inner diameter of about 2-4 nm and cross sectional diameter 3 to 5 nm. The lengths of the tubes are in the range of 500 nm to ~1 μm. The size of the obtained CNTs is found to be different from those reported so far in the literature. These nanotubes are having open ends and they are associated with roughly about 8 to 20 concentric cylinders. The observations
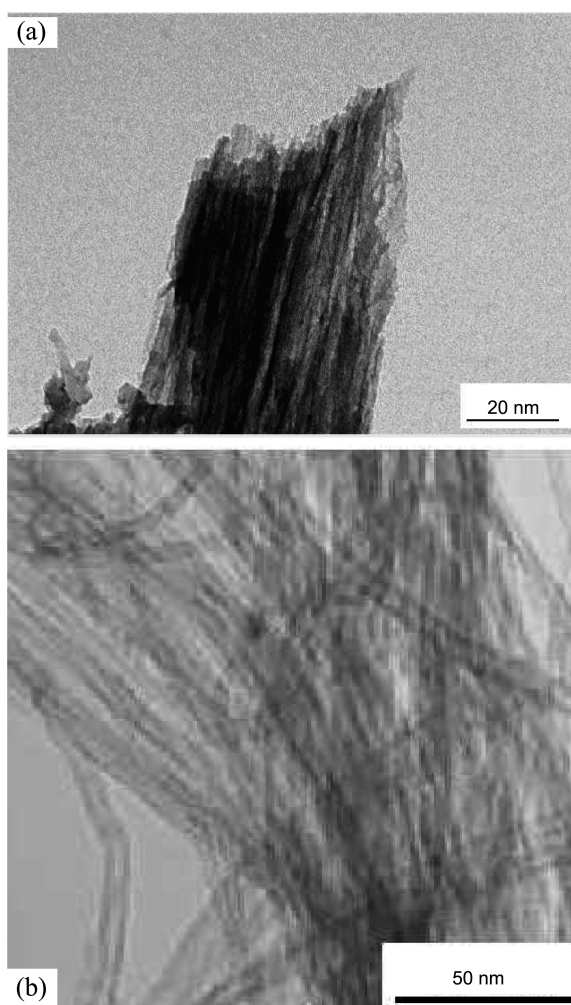

Figure 6. Raman spectrum of the as obtained product at optimum conditions.

High Yield Synthesis of Carbon Nanotube Bundles

Bull. Korean Chem. Soc. **2013**, Vol. 34, No. 10   3051

(a)

20 nm

(b)

50 nm

Figure 8. TEM images, (a) and (b) of the as-synthesized CNTs at optimum conditions showing the tubular structures.

(a)

5 nm

(b)

5 nm

Figure 9. High Resolution Transmission Electron Micrograph (HRTEM) images (a) and (b), of the CNTs.

have confirmed that tube ends were not found closed with Ni catalyst particles. The elemental analysis data of the sample synthesized at optimal conditions are found to be in good agreement with the calculated data. Experimentally. calculated.: C = 25.26%, H = 0%, N = 0%, calculated. data: C = 24.09%, H = 2.021%, N = 0.12%.

The mechanism of formation of the MWCNTs can be viewed to involve the freeing of C_2 units from the HCB by the reducing agent and assembling of these C_2 units into hexagonal carbon clusters. The diffusion of these clusters to the freshly reduced surface of the Ni particles and the nucleation takes place and further the process continues for the growth of cylindrical tubes along the axis of the cylinder. The growing wall which is the hexagonal sp^2 carbon lattice of the CNT will be favorable for the oriented growth of new hexagonal sp^2 carbon clusters due to their geometrical similarities.[21] In the growth of MWCNTs the outer wall stands stabilizing the inner wall, keeping it open for continuous growth.

With the help of BET analyzer, N_2 adsorption isotherm was measured at relative pressure (P/P$_0$, where P is the actual pressure of N_2 and P$_0$ is the saturated pressure of N_2 at
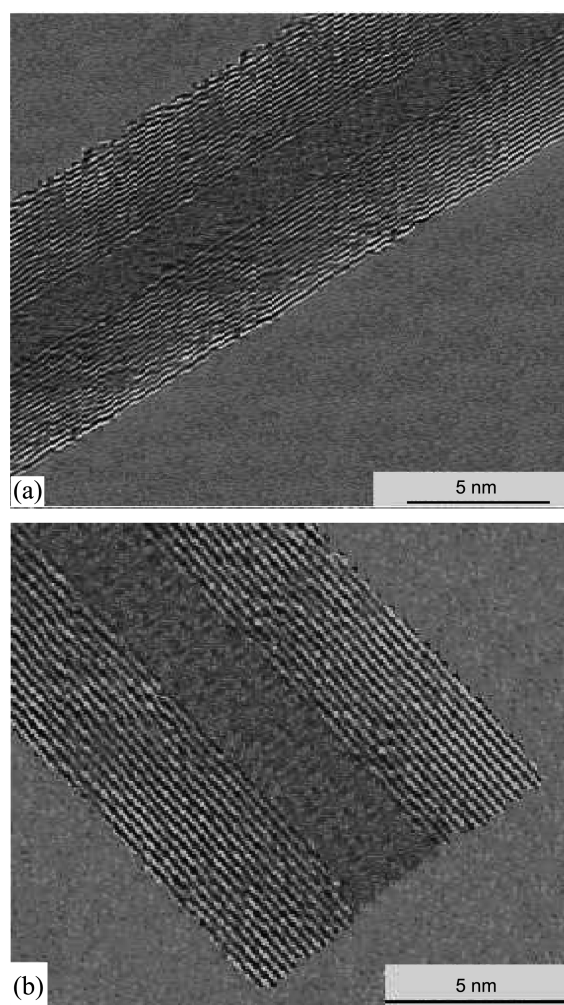
77 K) in the range of 0.0001 to 0.99. The adsorption data were then used to determine BET surface area by using BET equation.[28] Figure 10 shows the plot for N_2 adsorption for MWCNTs versus relative pressure (P/P$_0$). BET plot shown in figure is a straight line, having the slope and the intercept of the straight line as 0.1218 gcm^{-3} STP and 0.0016 gcm^{-3} STP respectively. From these values we had calculated the BET surface area of the sample as 35.25 m^{2}g^{-1} and Langmuir Surface Area found as 52.77 m^{2}g^{-1}. This value of surface area is higher than earlier reported value.[29]

$$v_m = \frac{1}{A+I} \qquad (1)$$

$$c = 1 + \frac{A}{I} \qquad (2)$$

From the formulae given above we had calculated BET monolayer volume and BET constant respectively. The values found as 8.09 cm^3/g STP and 74.91 respectively.

Nitrogen adsorption isotherms at 77 K for the purified MWNTs samples are shown in Figure 11. An adsorption isotherm is obtained by plotting a graph of the amount of gas
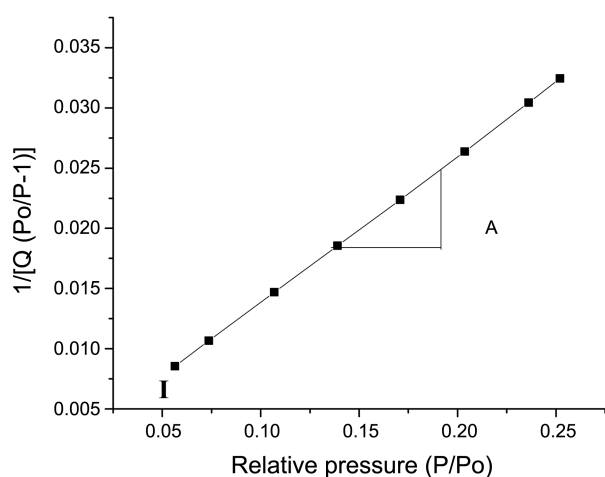
Figure 10. The linear graph between $1/[Q(Po/P\text{-}1)]$ against *P/Po*.
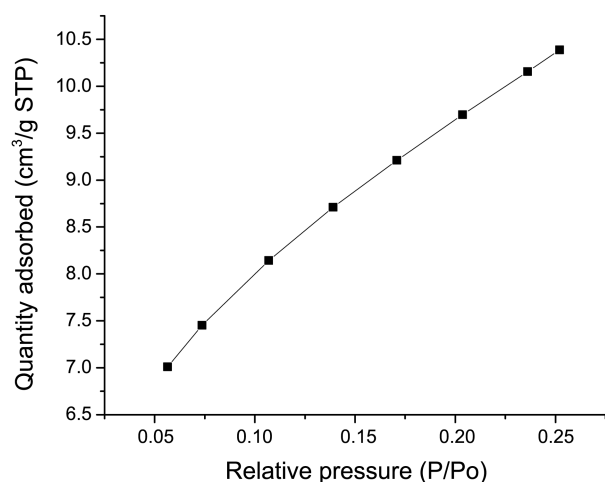

Figure 11. Graph between amount of gas adsorbed versus relative pressure belongs to II type isotherm.

adsorbed against relative pressure. MWNTs showed Type II adsorption isotherms. With the help of this graph we can explain that our CNTs product is powder with diameters exceeding micropores and the inflection point occurs near the completion of the first adsorbed monolayer.

Hydrogen Adsorption Studies. The storage of hydrogen can trust on physisorption because the adsorbed gas can be released reversibly. It follows multilayer mechanism if the adsorption takes place on an open surface and volume filling would happen in a pore narrower than 2 nm. Capillary condensation could happen if a pore size is in the range of 2 to 50 nm. Adsorption in a pore larger than 50 nm is the same as that on open surfaces. However, all the mechanisms here mentioned assume the hypothesis of condensation of the adsorbed gas (adsorbate). Such hypothesis does not survive at above-critical temperatures. The only mechanism for the adsorption of supercritical gases on any kind of adsorbents is the monolayer surface coverage of adsorbent. This possibility can be proved on studying the well-known BET theory of adsorption.[28]

Here, we focus on the adsorption of two types of gases,

nitrogen and hydrogen gas onto the carbon nanotubes. Nitrogen gas is widely used for the determination of the surface area of the samples referred as the BET method, which we had discussed already. We had studied H_2 gas adsorption on our CNTs sample based on N_2 adsorption studies, by presenting a simple empirical model where condensation of hydrogen as a monolayer on the surface of nanotubes as well as bulk condensation in the cavity of the tube is assumed as discussed above.[30]

The condensation of a monolayer of hydrogen on a graphene sheet with a specific surface area of $S1 = 1315 \text{ m}^2\text{g}^{-1}$ leads to

$$\frac{m(H2)}{m(C)} = \frac{S1\,Mad}{Sm\,Na} \tag{3}$$

Where *Mad* stands for the molecular mass of the adsorbate *Sm* stands for surface area occupied by each molecule and *Na* for the Avogadro constant ($Na = 6.0220 \times 10^{23} \text{ mol}^{-1}$). *Sm* can be calculated by knowing the *dm*, diameter of the spherical molecule.

$$Sm = \frac{\sqrt{3}}{2}(dm)^2 \tag{4}$$

If we know the quantity of adsorbate in the monolayer during adsorption we can find the *dm* of the molecule. Volume of the molecule can be calculated by

$$Vad = \frac{Mad}{\rho ad\,Na} \tag{5}$$

Where *rad* for the density of the liquid adsorbate. *Vad* represents volume reserved for each molecule in the liquid. Assuming that molecules are spherical and closed-packed the volume of the sphere representing the molecule is by a factor of 0.7405 smaller than v_{ad}.

$$Vm = \frac{\pi}{3\sqrt{2}},\ Vad = \frac{\pi}{3\sqrt{2}},\ Mad/\rho ad\,Na \tag{6}$$

By knowing the value of *Vm* we can calculate the *dm* by assuming a close packing of molecules in a two dimensional layer at the surface.

$$dm = \frac{\sqrt[3]{6Vm}}{\pi} = \sqrt[3]{2}\,Mad/\rho ad\,Na \tag{7}$$

So with the help of Eq. (8) *Sm* can be rewrite as

$$Sm = \frac{\sqrt{3}}{2}\left(\sqrt{2}\frac{Mad}{\rho ad\,Na}\right) \tag{8}$$

So in order to calculate the *Vm*, *dm* and *Sm* by the equation from (5) to (8), we used *Mad* and ρ values of the adsorbate and tabulated these properties in Table 2.

But for the carbon nanotubes where diameter does not exceed from few nm, the potential fields from opposite walls will overlap so that the attractive force acting on adsorbate molecules will be increased as compared with that on an open surface resulting in the higher adsorption of H_2 molecules inside the nanotubes compared to the flat surface of graphite. If we presume a condensation of the hydrogen gas

Table 3. Properties of Nitrogen and Hydrogen gas

Property	N_2	H_2
Mad (gmol^{-1})	28.0140	2.0159
ρ (gcm^{-3})	0.8070	0.0708
Vm (nm^{-3})	0.042	0.0350
dm (nm)	0.4336	0.4059
Sm (nm^{-2})	0.1477	0.1294

in the cavity of a nanotube, we can represent the ratio of the mass of hydrogen to the mass of carbon as

$$\frac{m(H2)}{m(C)} = S1\, dnt\rho ad/4 \qquad (9)$$

We had calculated this ratio for our sample having CNTs with diameter ~10 nm is m (H$_2$)/m(C) = 0.0208. Where *S*1 is the specific surface area for the CNT sample calculated with the help of S (form BET) as,

$$H2(mass\%) = \frac{m(H2)}{m(H2)+m(C)} \times 100$$

$$= \frac{1}{1+\left(\dfrac{m(C)}{m(H2)}\right)} \times 100 \qquad (10)$$

that results in 2.03%.

Conclusion

We have successfully synthesized the well-ordered bundles of carbon nanotubes by solvothermal route at very low temperature of 180 ºC in high yield of about 70-75%. The CNTs thus obtained are having significant dimensions, that too being multiwalled tubes. The CNTs are long and straight with outer diameter of about 5-9 nm, the inner diameter 2-4 nm, cross sectional diameter up to 5 nm and length from about 500 nm up to about 1ìm. Employing the BET surface area study, BET and Langmuir surface areas are calculated. The values are 35.25 m^2/g and 52.77 m^2/g respectively which are of considerably good significance. The calculated amount of hydrogen adsorbed to be 2.03% by considering the condensation of hydrogen as a monolayer at the surface of nanotubes as well as bulk condensation in the cavity of the tube. In the synthesis of CNTs bundles temperature and catalyst amount play an important role. The observation and results present that the optimum temperature is 180 ºC, below that no CNT formation took place and above that temperature no significant changes observed. Amount of catalyst also has a significance effect on the % yield of the product. 0.1 gm of the catalyst is optimum for CNTs synthesis. Thus this research work provides an efficient procedure for the synthesis of MWCNTs of significant dimensions in high yield at low temperature with good surface area and H$_2$ storage capacity.

References

1. Iijima, S. *Nature* **1991**, *354*, 56.
2. Shim, M.; Javey, A.; Kam N. W. S.; Dai, H. J. *J. Am. Chem. Soc.* **2001**, *123*, 11512.
3. Kong, J.; Franklin, N. R.; Zhou, C.; Chapline, M. G.; Peng, S.; Cho, K.; Dai, H. *Science* **2000**, *287*, 622.
4. Collins, P. G.; Zettl, A.; Bando, H.; Smalley, R. E. *Science* **1997**, *278*, 100.
5. Arenillas, A.; Zubizarreta, L.; Pis, J. J. *Int. J. Hydrogen Energy* **2009**, *34*, 4575.
6. Baughman, R. H.; Cui, C. X.; Zakhidov, A. A.; Iqbal, Z.; Barisci, J. N.; Spinks, G. M.; Wallace, G. G.; Mazzoldi, A.; De Rossi, D.; Rinzler, A. G.; Jaschinski, O.; Roth, S.; Kertesz, M. *Science* **1999**, *284*, 1340.
7. Kim, P.; Lieber, C. M. *Science* **1999**, *286*, 2148.
8. Fan, S. S.; Chapline, M. G.; Franklin, N. R.; Tombler, T. W.; Cassell, A. M.; Dai, H. J. *Science* **1999**, *283*, 512.
9. Peigney, A.; Coquay, P.; Flahaut, E.; Vandenberghe, R. E.; De Grave, E.; Laurent, C. *J. Phys. Chem. B* **2001**, *105*, 9699.
10. Kasumov, Y. A.; Shailos, A.; Khodos1, I. I.; Volkov, V. T.; Levashov, V. I.; Matveev, V. N.; Gueron, S.; Kobylko, M.; Kociak, M.; Bouchiat, V.; Agache, V.; Rollier, A. S.; Uchaillot, L.; Bonnot, A. M.; Kasumov, A. Y. *Appl. Phys. A* **2007**, *88*, 687.
11. Bethune, D. S.; Kiang, C. H.; deVries, M. S.; Gorman, G.; Savoy, R.; Vazquez, J.; Beyers, R. *Nature* **1993**, *363*, 605.
12. Scott, C. D.; Arepalli, S.; Nikolaev, P.; Smalley, R. E. *Appl. Phys. A* **2001**, *72*, 573.
13. Guerrero, A.; Puerta, J.; Gomez, F.; Blanco, F. *Phys. Scr.* **2008**, *131*, 4007.
14. Joseyacaman, M.; Mikyoshida, M.; Rendon, L.; Santiesteban, J. G. *Appl. Phys. Lett.* **1993**, *62*, 657.
15. Endo, M.; Takeuchi, K.; Igarashi, S.; Kobori, K.; Minoru, S. K.; Kroto, H. W. *J. Phys. Chem. Solids* **1993**, *54*, 1841.
16. Mahanandia, P.; Vishwakarma, P. N.; Nanda, K. K.; Prasad, V.; Baraic, K.; Mondal, A. K.; Sarangi, S.; Dey, G. K.; Subramanyam, S. V. *Solid State Commun.* **2008**, *145*, 143.
17. Cmoreno, J. M.; Yoshimura, M. *J. Am. Chem. Soc.* **2001**, *123*, 741.
18. O'Loughlin, J. K.; Kiang, C. H.; Wallace, C. H.; Reynolds, T. K.; Rao, L.; Kaner, R. B. *J. Phys. Chem. B* **2001**, *105*, 1921.
19. Mack, J. J.; Tari, S.; Kaner, R. B. *Inorg. Chem.* **2006**, *45*, 4243.
20. Jiang, Y.; Wu, Y.; Zhang, S. Y.; Xu, C. Y.; Yu, W. C.; Xie, Y.; Qian, Y. T. *J. Am. Chem. Soc.* **2000**, *122*, 12383.
21. Wang, X. J.; Lu, J.; Xie,Y.; Du, G.; Guo, Q. X.; Zhang, S. Y. *J. Phys. Chem. B* **2002**, *106*, 933.
22. Lee, C. Y.; Chiu, H. T.; Peng, C. W.; Yen, M. Y.; Cang, Y. H.; Liu, C. S. *Adv. Mater.* **2001**, *13*, 1105-1107.
23. Liu, J.; Shao, M.; Chen, X.; Yu, W.; Liu, X.; Qian, Y. *J. Am. Chem. Soc.* **2003**, *125*, 8088.
24. Wang, W.; Kunwar, S.; Huang, J. Y.; Wang, D. Z.; Ren, Z. F. *Nanotech.* **2005**, *16*, 21.
25. Liu, J.; Shao, M.; Tang, Q.; Zhang, S.; Qian, Y. *J. Phys. Chem. B* **2003**, *107*, 6329.
26. Cheng, J.; Zhang, X.; Luo, Z.; Liu, F.; Ye, Y.; Yin, W.; Liu, W.; Han, Y. *Mater. Chem. Phys.* **2006**, *95*, 5.

27. Costa, S.; Borowiak-Palen, E.; Kruszyñska, M.; Bachmatiuk, A.; Kalenczuk, R. J. *Mater Sci-Poland.* **2008**, *26*, 433-441.

28. Brunauer, S.; Emmett, P. H.; Teller, E. *J. Am. Chem. Soc.* **1930**, *60*, 309.

29. Tsang, S. C.; Harris, P. J. F.; Green, M. L. H. *Nature* **1993**, *362*, 520.

30. Zuttel, A.; Sudan, P.; Mauron, P.; Wenger, P. *Applied Physics A* **2004**, *78*, 941.